

Electronic Supplementary Information

Tuning the photophysical properties of carboranyl luminophores by *closo-* to *nido-*carborane conversion and application to OFF-ON fluoride sensing

Nguyen Van Nghia,^{a,b} Jihun Oh,^a Surendran Sujith,^a Jaehoon Jung*^a and Min Hyung Lee*^a

^a Department of Chemistry, University of Ulsan, Ulsan 44610, Republic of Korea

^b Institute of Research and Development, Duy Tan University, Da Nang 550000, Vietnam

Contents

1. Experimental data.....	S2
2. Computational details.....	S14

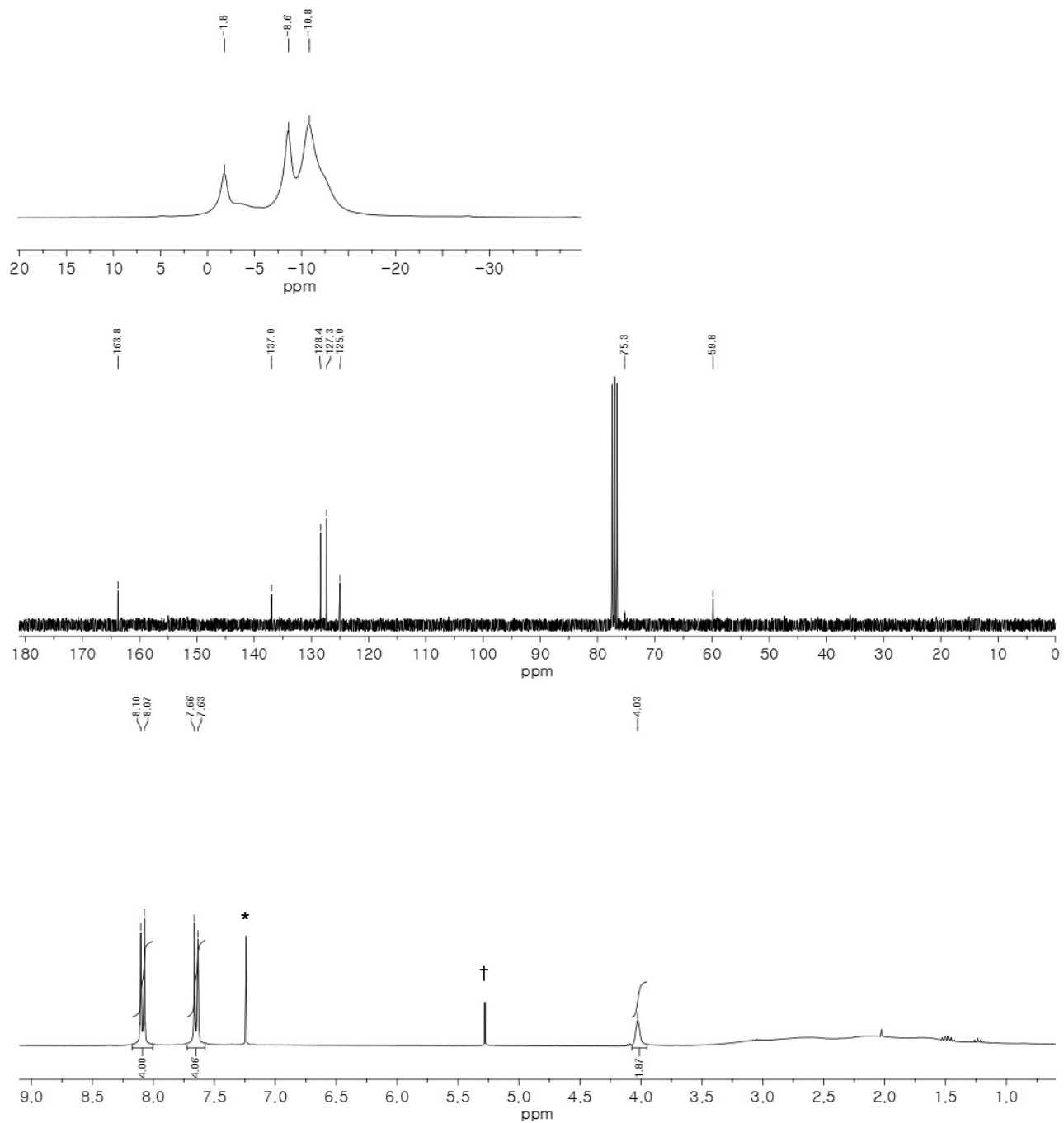


Fig. S1. ^{11}B (top), ^{13}C (middle), and ^1H (bottom) NMR spectra of *closo*-OXD1 (* and † from CDCl_3 and CH_2Cl_2 , respectively).

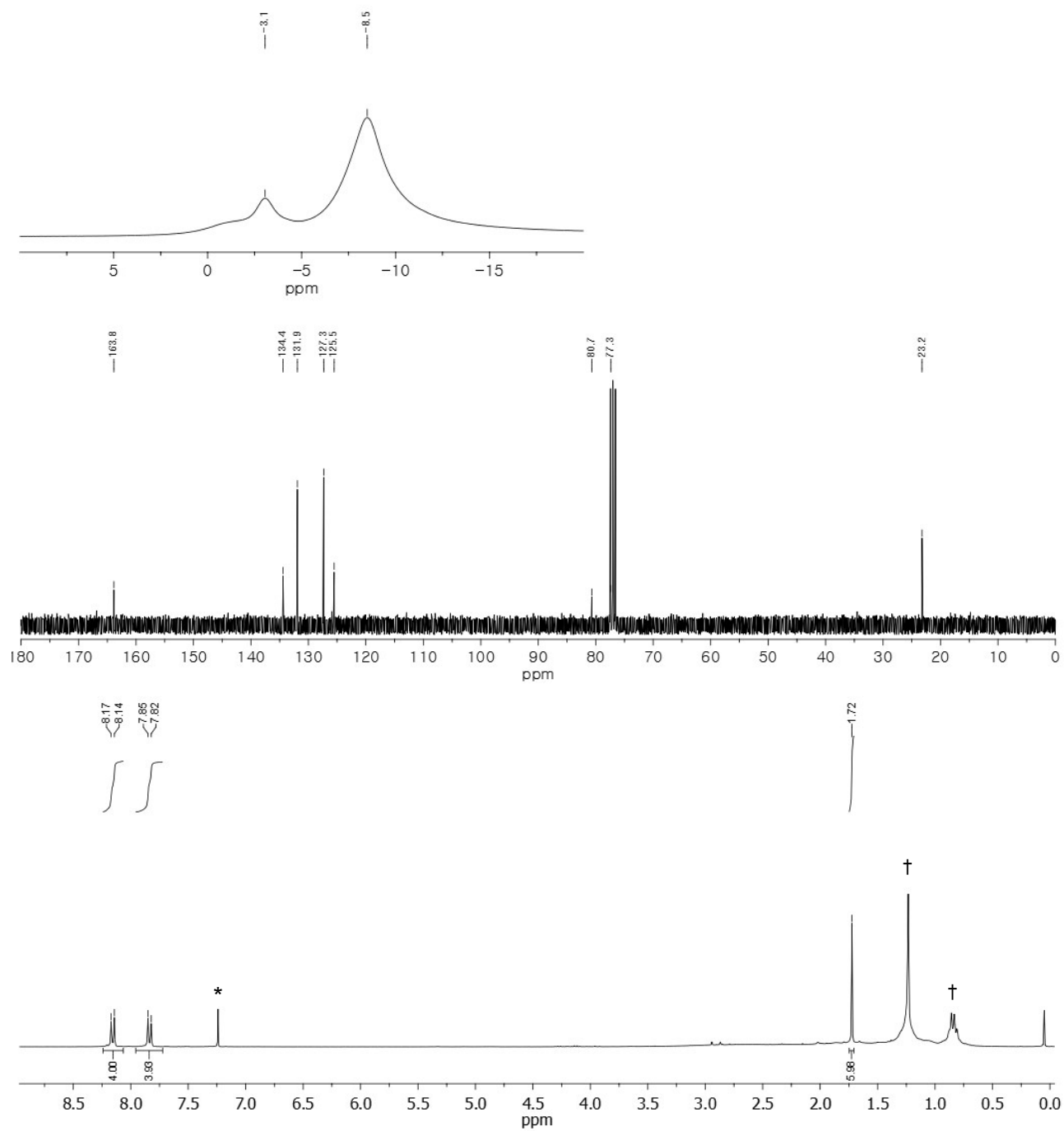


Fig. S2. ^{11}B (top), ^{13}C (middle), and ^1H (bottom) NMR spectra of *closo-OXD2* (* and † from CDCl_3 and *n*-hexane, respectively).

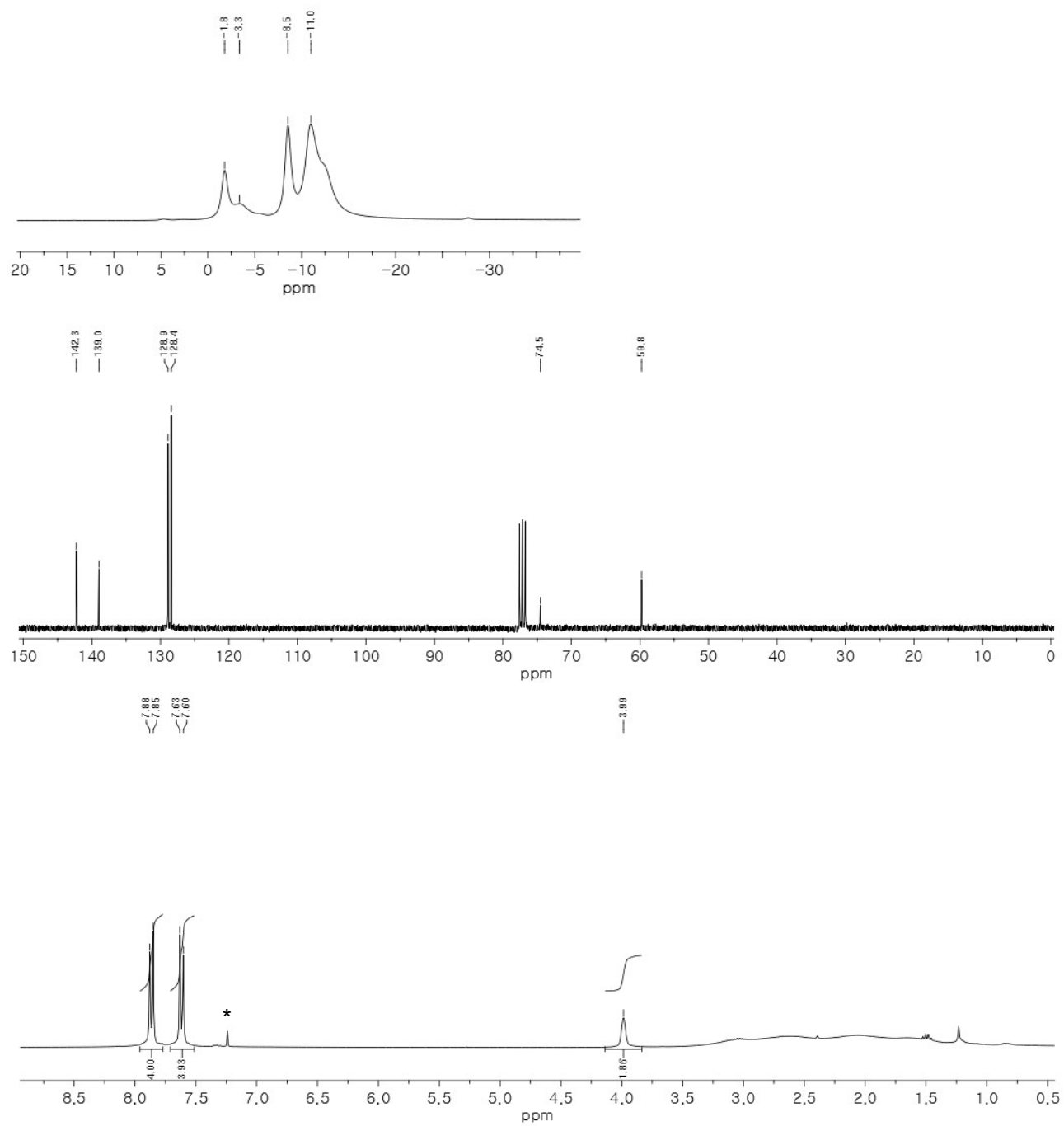


Fig. S3. ^{11}B (top), ^{13}C (middle), and ^1H (bottom) NMR spectra of *closo-DPS1* (* from CDCl_3).

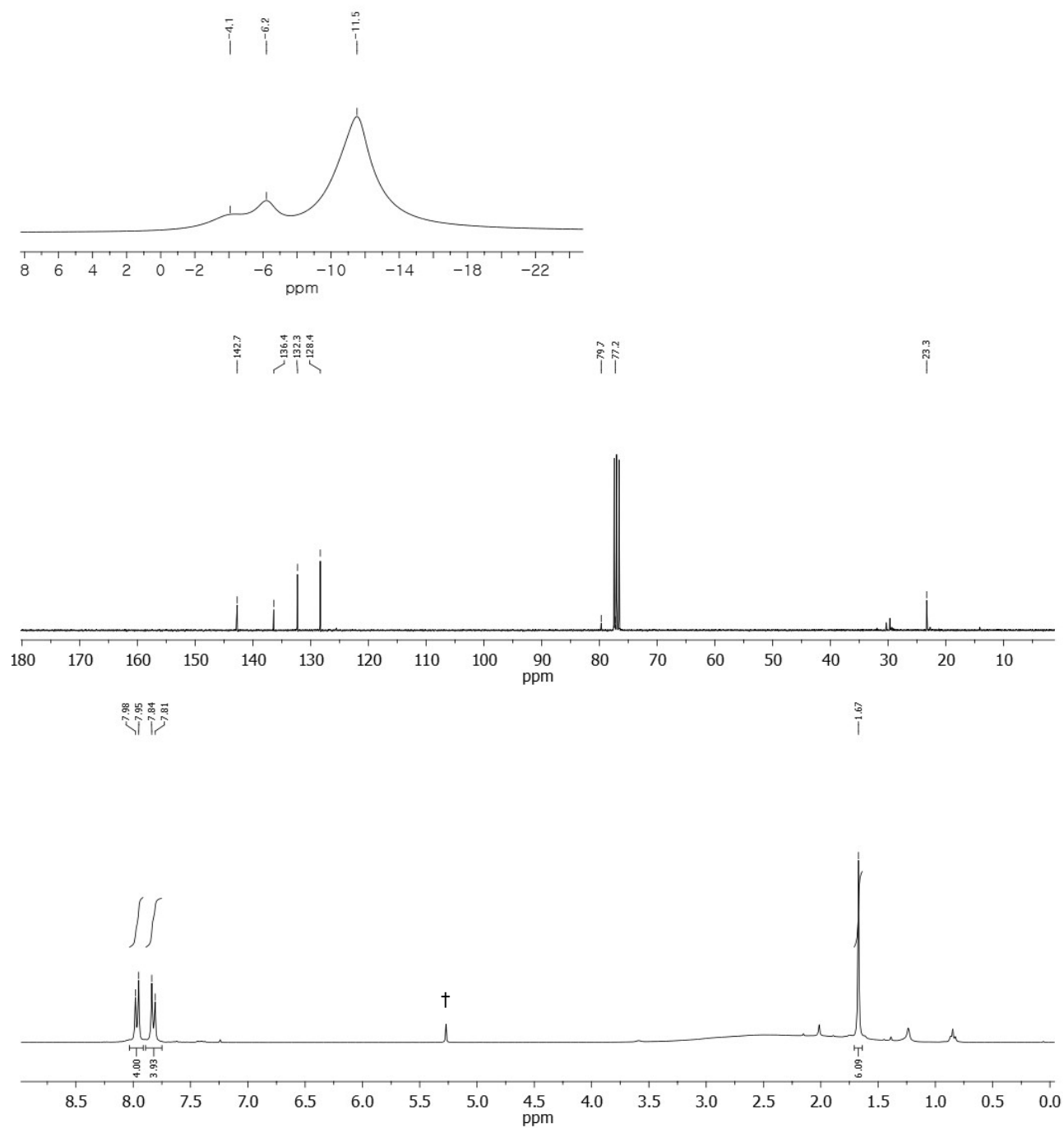


Fig. S4. ¹¹B (top), ¹³C (middle), and ¹H (bottom) NMR spectra of *closo-DPS2* († from CH₂Cl₂).

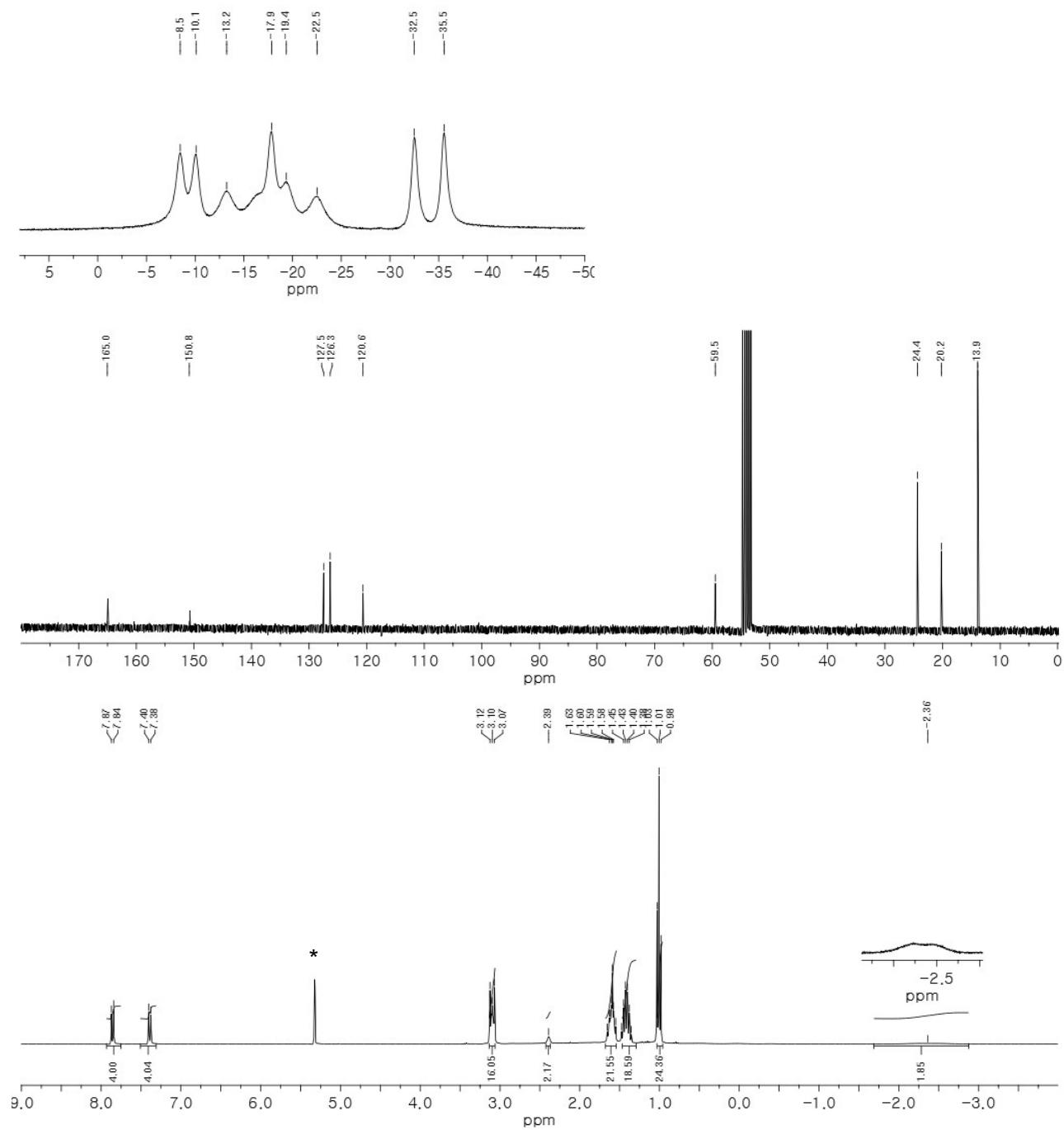


Fig. S5. ¹¹B (top), ¹³C (middle), and ¹H (bottom) NMR spectra of *nido*-OXD1 (* from CD₂Cl₂).

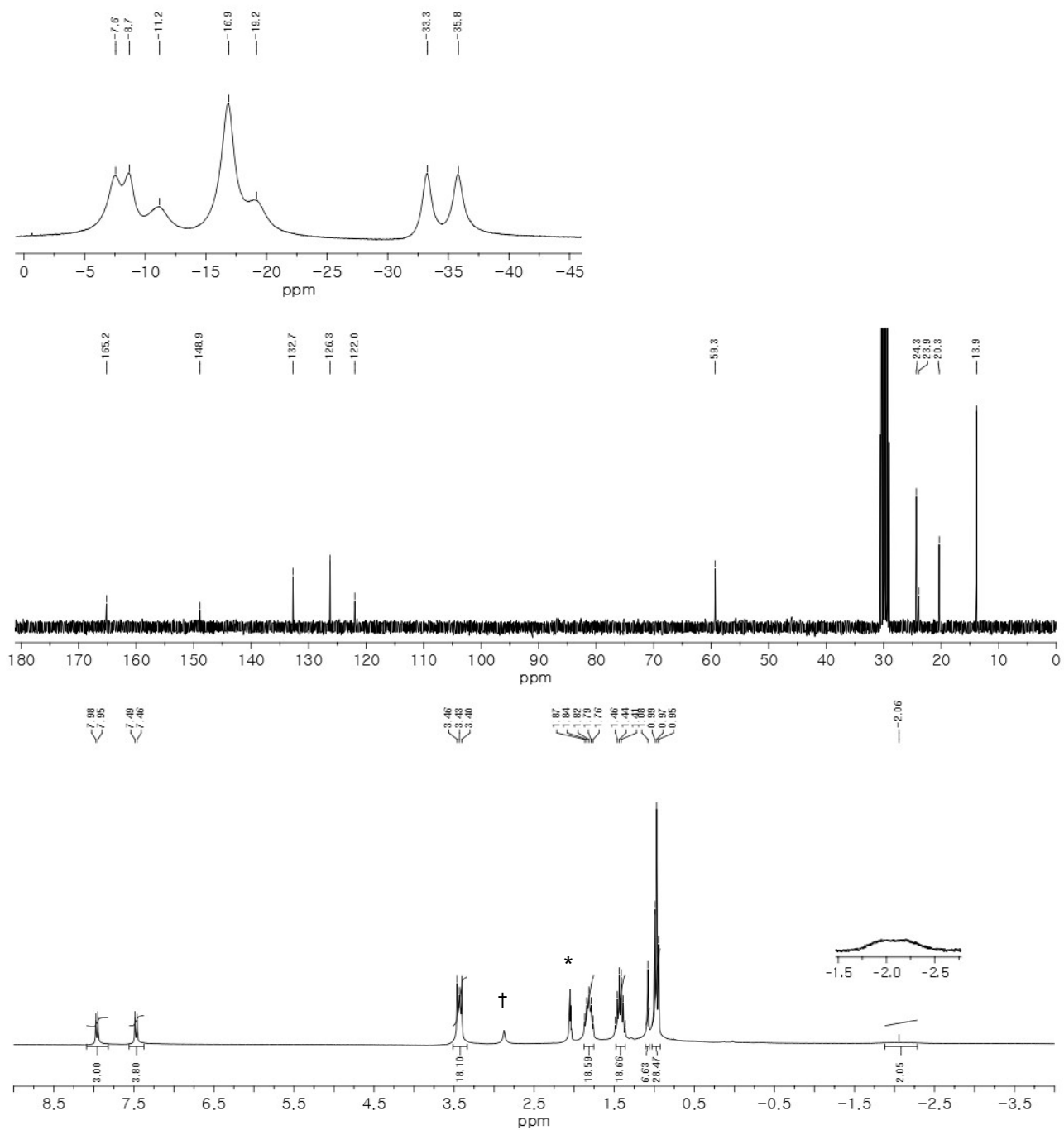


Fig. S6. ^{11}B (top), ^{13}C (middle), and ^1H (bottom) NMR spectra of *nido*-OXD2 (* and † from acetone- d_6 and H_2O , respectively).

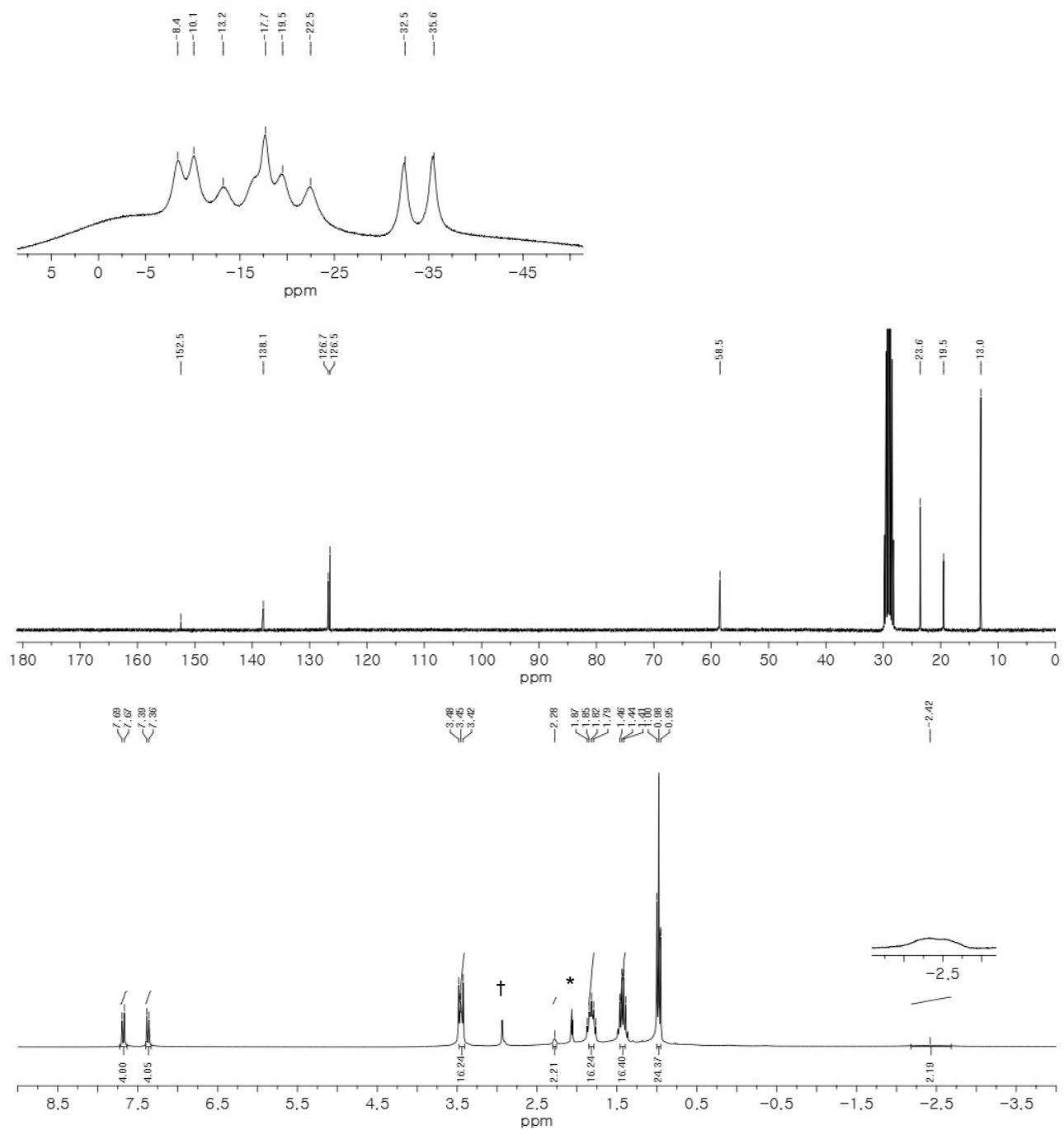


Fig. S7. ¹¹B (top), ¹³C (middle), and ¹H (bottom) NMR spectra of *nido*-DPS1 (* and † from acetone-*d*₆ and H₂O, respectively).

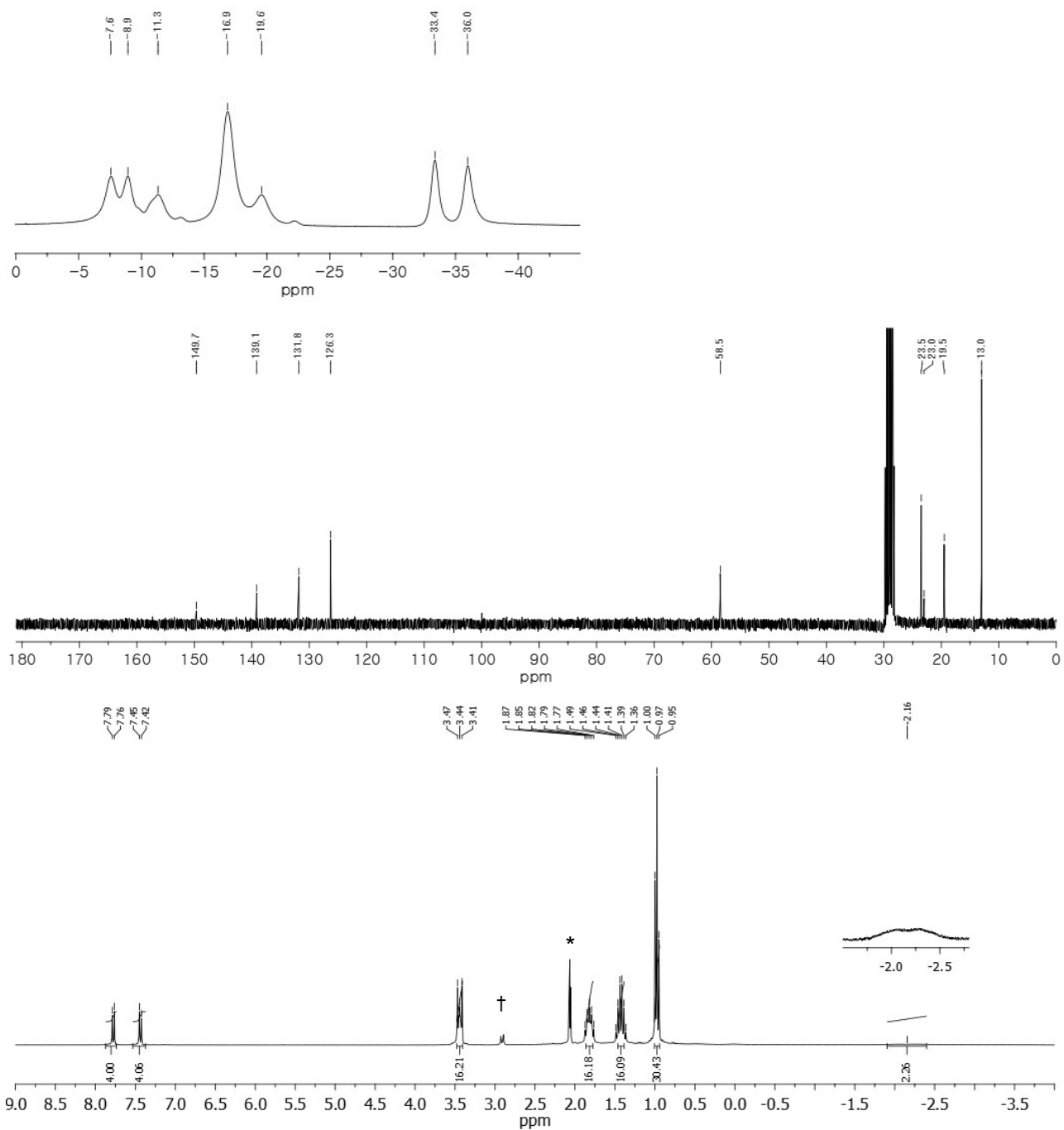


Fig. S8. ¹¹B (top), ¹³C (middle), and ¹H (bottom) NMR spectra of *nido*-DPS2 (* and † from acetone-*d*₆ and H₂O, respectively).

Table S1. Crystallographic data and parameters for *closo-OXD1*.

	<i>closo-OXD1</i>
formula	C ₁₈ H ₃₀ B ₂₀ N ₂ O
formula weight	506.64
crystal system	Monoclinic
space group	<i>P</i> 2 ₁ / <i>n</i>
<i>a</i> (Å)	12.56330(10)
<i>b</i> (Å)	12.09970(10)
<i>c</i> (Å)	18.4978(2)
α (°)	90
β (°)	97.7708(6)
γ (°)	90
<i>V</i> (Å ³)	2786.07(4)
<i>Z</i>	4
ρ_{calc} (g cm ⁻³)	1.208
μ (mm ⁻¹)	0.062
<i>F</i> (000)	1040
<i>T</i> (K)	173(2)
<i>hkl</i> range	-16 → +16, -12 → +16, -24 → +24
measd reflns	27843
unique reflns [<i>R</i> _{int}]	6868 [0.0327]
reflns used for refinement	6868
refined parameters	370
<i>R</i> 1 ^{<i>a</i>} (<i>I</i> > 2σ(<i>I</i>))	0.0539
w <i>R</i> 2 ^{<i>b</i>} all data	0.1556
GOF on <i>F</i> ²	1.041
ρ_{fin} (max/min) (e Å ⁻³)	0.381/-0.336

^{*a*} $R1 = \sum ||F_o| - |F_c|| / \sum |F_o|$. ^{*b*} $wR2 = \{[\sum w(F_o^2 - F_c^2)^2] / [\sum w(F_o^2)^2]\}^{1/2}$.

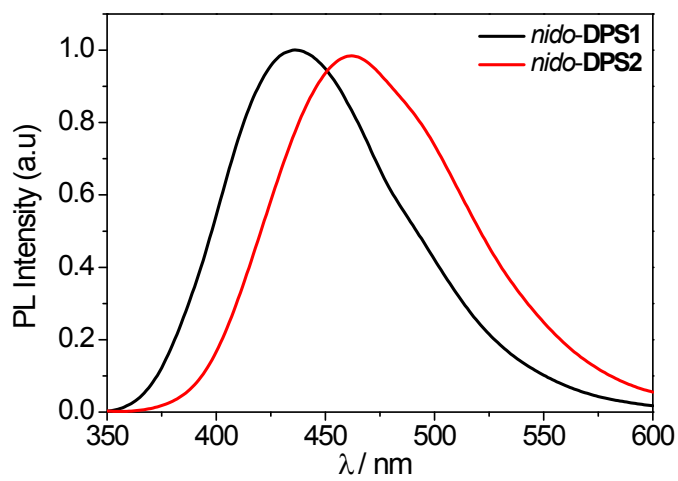
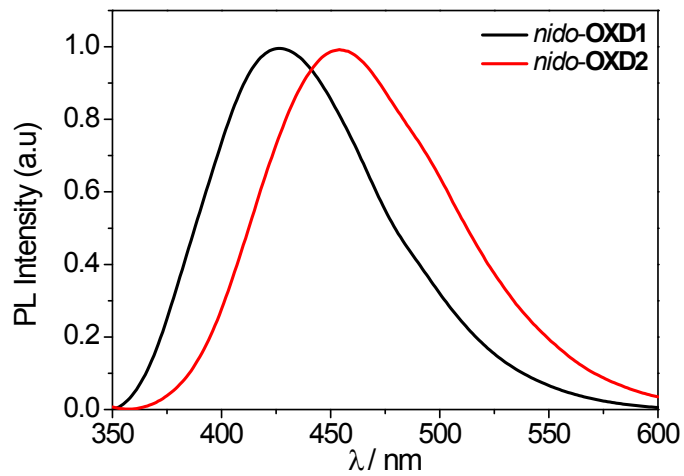


Fig. S9. PL spectra of (top) *nido*-OXD1–2 and (bottom) *nido*-DPS1–2 in 10 wt%-doped PMMA film.

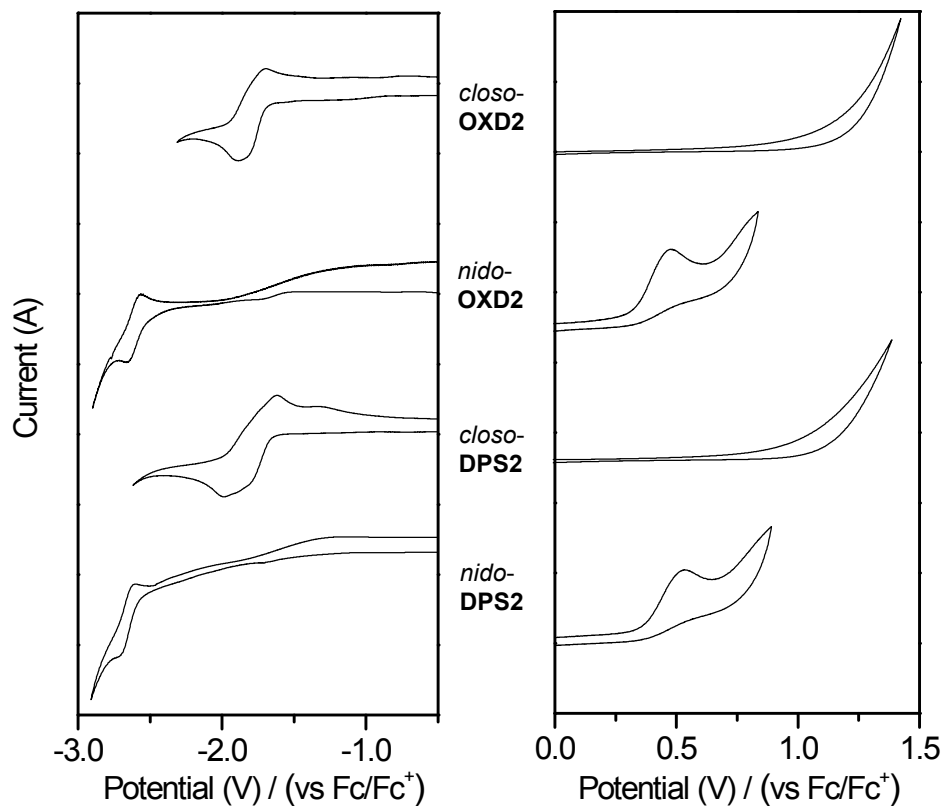


Fig. S10. Cyclic voltammograms of *closo*/*nido*-OXD2 and *closo*/*nido*-DPS2 showing reduction (left) and oxidation (right) (1.0×10^{-3} M in DMF except for reduction of *nido*-DPS2 (MeCN), scan rate = 100–200 mV/s).

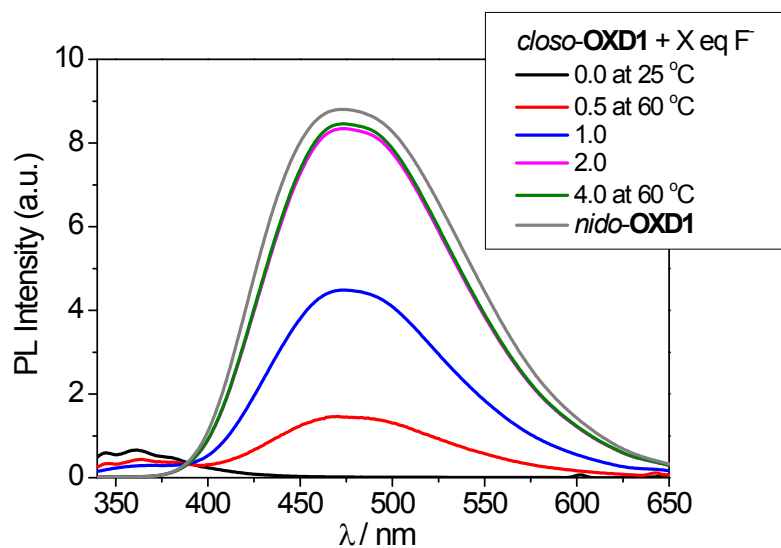


Fig. S11. Spectral change in the fluorescence of *closo-OXD1* (2×10^{-5} M in THF) in the presence of different amounts of fluoride after heating at 60 °C for 2 h ($\lambda_{\text{ex}} = 320$ nm).

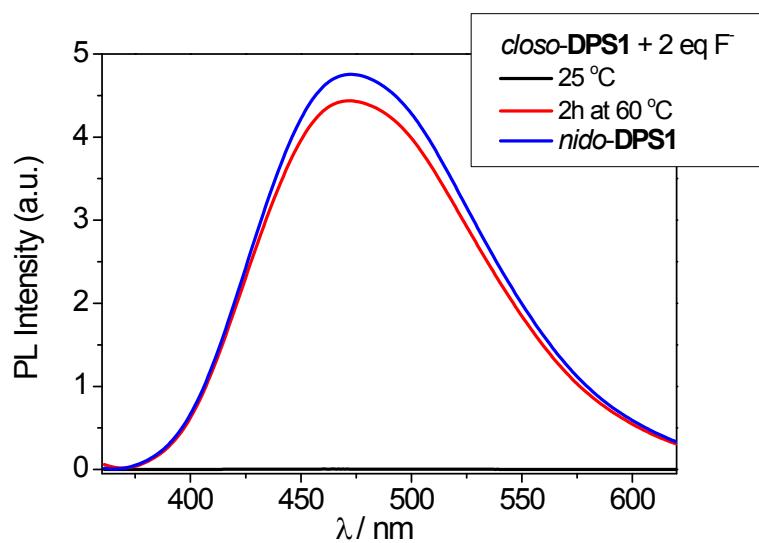


Fig. S12. Spectral change in the fluorescence of *closo-DPS1* (2×10^{-5} M in THF) in the presence of 2 equiv of fluoride at 60 °C for 2 h ($\lambda_{\text{ex}} = 320$ nm).

Computational Details

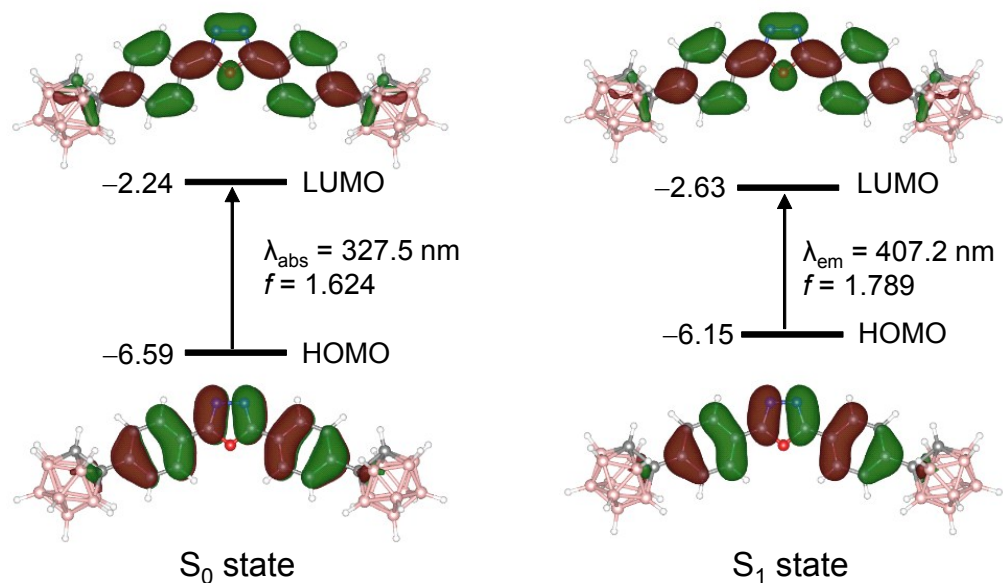


Fig. S13. Frontier molecular orbital diagrams and energies (eV) from DFT calculation (PCM in THF) of *closo*-OXD1 (left) in the ground state (S₀) and (right) in the lowest singlet excited state (S₁) geometries. The transition energy (in nm) was calculated using the TD-B3LYP method.

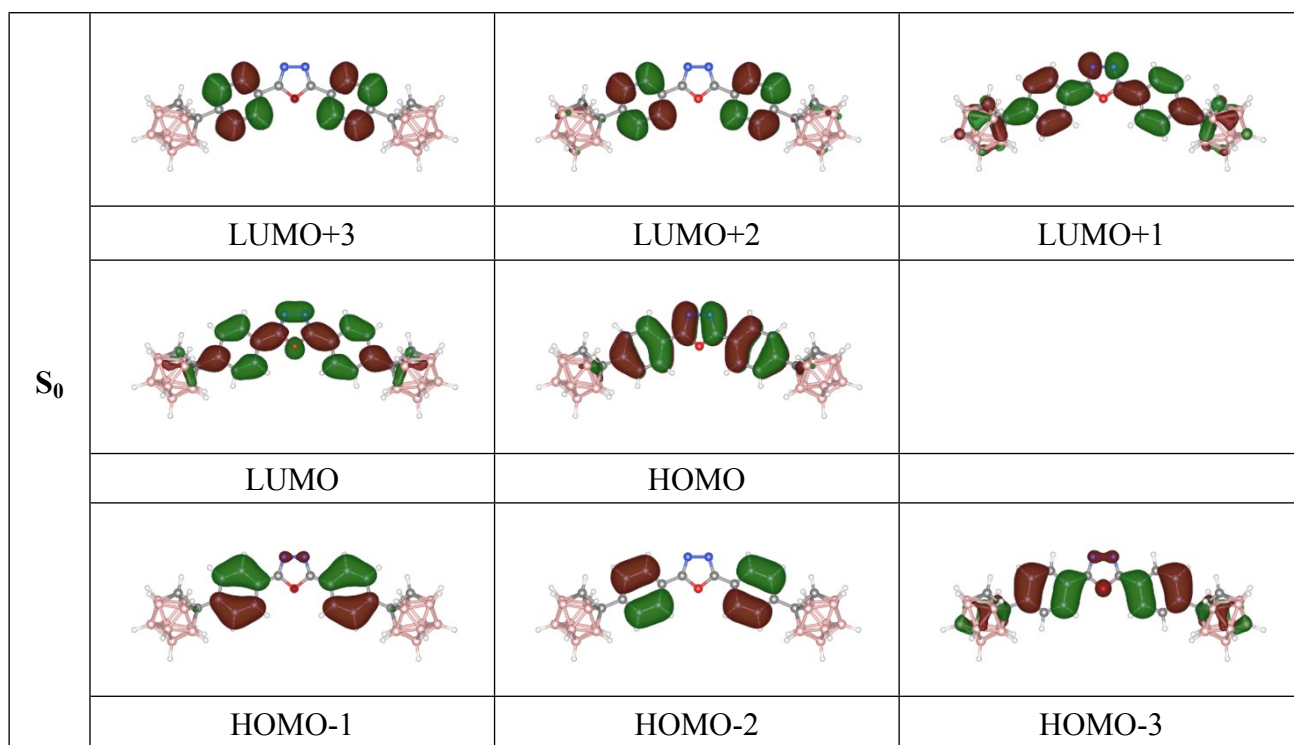


Fig. S14. Frontier molecular orbitals of *closo*-OXD1 from IEFPCM-TD-B3LYP calculations (solvent: THF) at the ground state (S_0) optimized geometry (isovalue = 0.02).

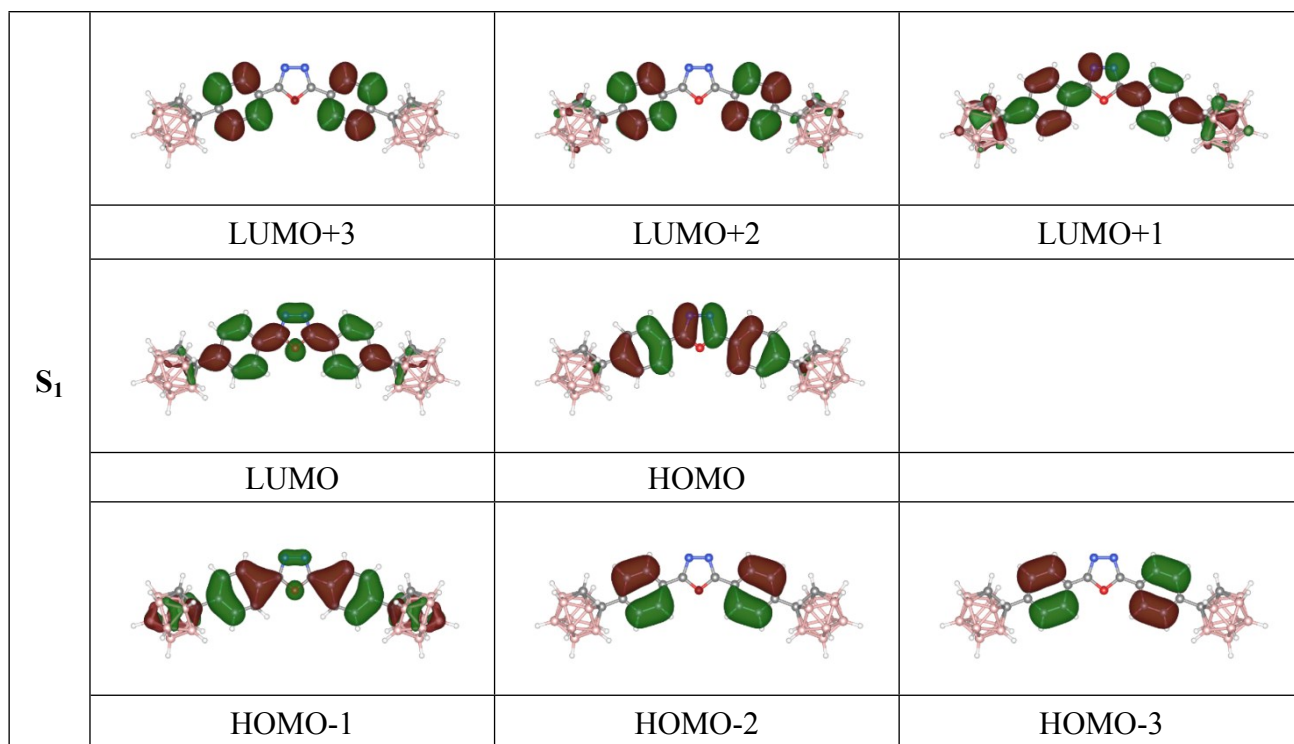


Fig. S15. Frontier molecular orbitals of *closo*-OXD1 from IEFPCM-TD-B3LYP calculations (solvent: THF) at the lowest singlet excited state (S_1) optimized geometry (isovalue = 0.02).

Table S2. Molecular orbital energies (in eV) and contributions of moieties (in %) for *closo-OXD1* from IEFPCM-B3LYP calculations (solvent: THF) at the ground state (S_0) optimized geometry.

MO	Energy	OXD	Phenylene	<i>closo</i> -CB
LUMO+3	-0.85	0.15	92.18	7.67
LUMO+2	-0.87	0.41	89.96	9.63
LUMO+1	-1.58	23.16	59.69	17.15
LUMO	-2.24	32.60	58.10	9.29
HOMO	-6.59	37.55	56.60	5.85
HOMO-1	-7.58	1.67	93.34	4.99
HOMO-2	-7.60	0.11	98.71	1.19
HOMO-3	-7.62	4.15	83.73	12.13

Table S3. Molecular orbital energies (in eV) and contributions of moieties (in %) for *closo-OXD1* from IEFPCM-TD-B3LYP calculations (solvent: THF) at the lowest singlet excited state (S_1) optimized geometry.

MO	Energy	OXD	Phenylene	<i>closo</i> -CB
LUMO+3	-0.78	0.15	90.79	9.07
LUMO+2	-0.81	0.59	87.91	11.50
LUMO+1	-1.67	26.85	57.12	16.03
LUMO	-2.63	34.99	56.96	8.05
HOMO	-6.15	40.98	53.71	5.32
HOMO-1	-7.56	7.75	77.12	15.13
HOMO-2	-7.66	0.25	98.36	1.39
HOMO-3	-7.67	0.21	98.56	1.24

Table S4. Computed absorption and emission wavelengths ($\lambda_{\text{calc.}}$ in nm) and oscillator strengths ($f_{\text{calc.}}$) for *closo-OXD1* from IEFPCM-TD-B3LYP calculations at the ground (S_0) and lowest singlet excited state (S_1) optimized geometries.

Transition	$\lambda_{\text{calc.}}$ /nm	$f_{\text{calc.}}$	Major contribution
$S_0 \rightarrow S_1$	327.5	1.624	HOMO \rightarrow LUMO (99%)
$S_0 \rightarrow S_2$	269.6	0.078	HOMO \rightarrow LUMO+1 (64%), HOMO-1 \rightarrow LUMO (26%)
$S_0 \rightarrow S_3$	266.6	0.000	HOMO-2 \rightarrow LUMO (69%), HOMO \rightarrow LUMO+3 (21%)
$S_0 \rightarrow S_4$	266.0	0.001	HOMO-1 \rightarrow LUMO (29%), HOMO \rightarrow LUMO+1 (25%), HOMO-3 \rightarrow LUMO (23%), HOMO \rightarrow LUMO+2 (16%)
$S_1 \rightarrow S_0$	407.2 (364.5) ^a	1.789	HOMO \rightarrow LUMO (99%)

^a For the adiabatic transition corresponding to the 0–0 fluorescence.

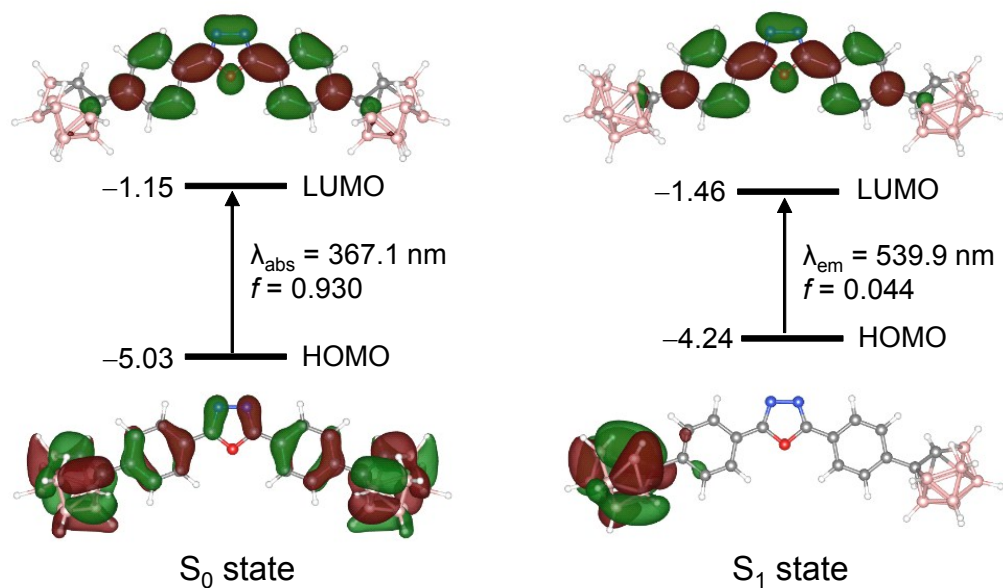


Fig. S16. Frontier molecular orbital diagrams and energies (eV) from DFT calculation (PCM in THF) of *nido*-OXD1 (left) in the ground state (S_0) and (right) in the lowest singlet excited state (S_1) geometries. The transition energy (in nm) was calculated using the TD-B3LYP method.

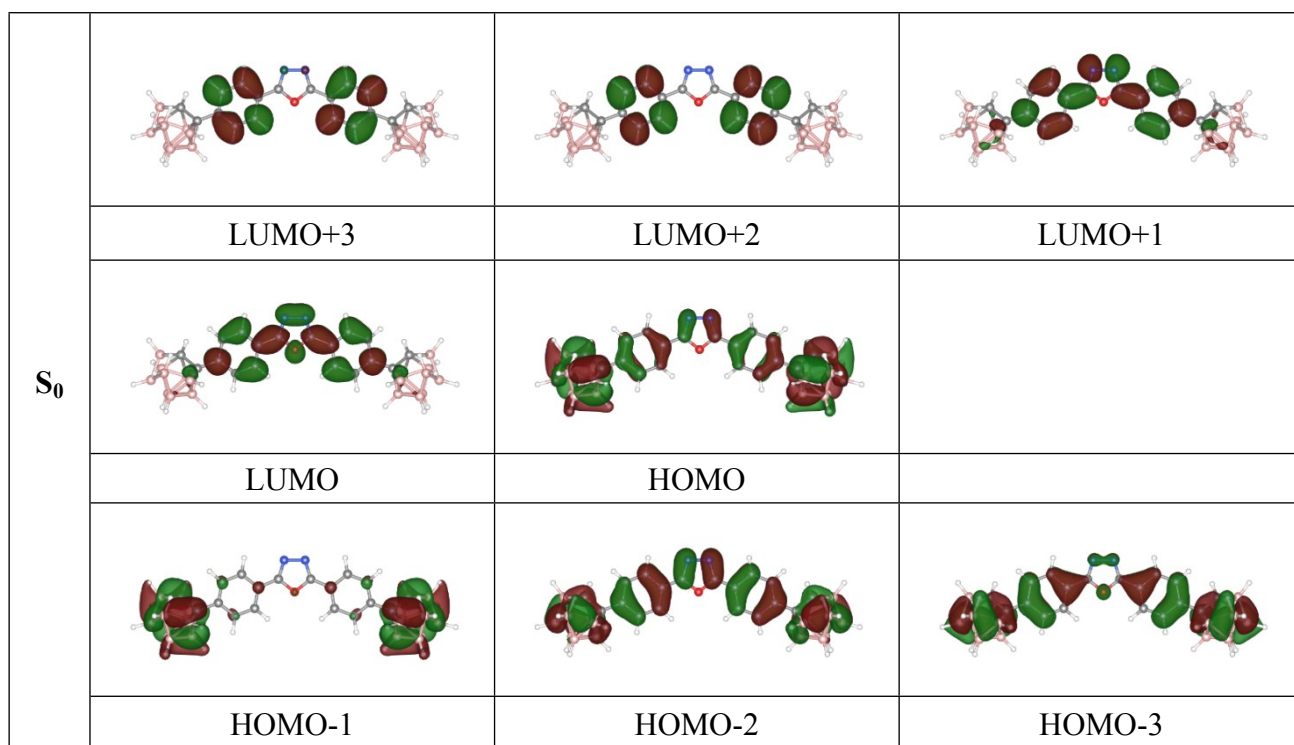


Fig. S17. Frontier molecular orbitals of *nido-OXD1* from IEFPCM-TD-B3LYP calculations (solvent: THF) at the ground state (S_0) optimized geometry (isovalue = 0.02).

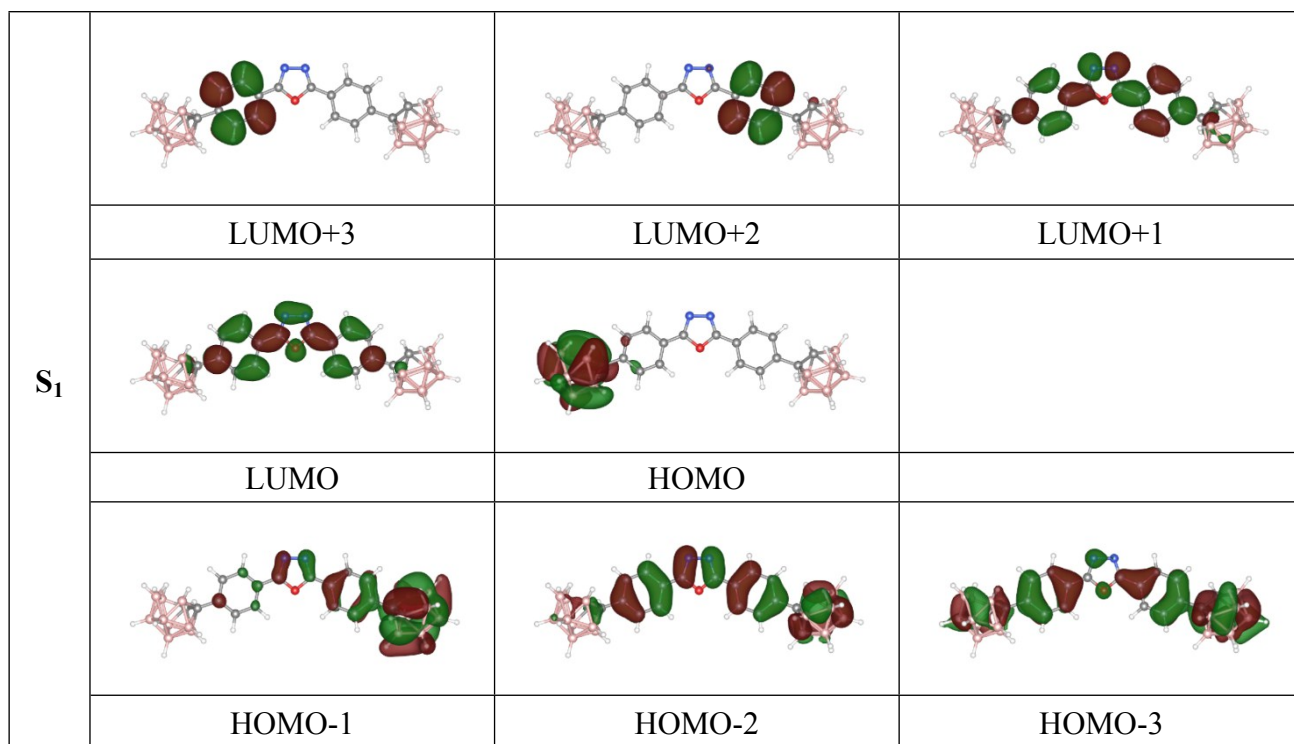


Fig. S18. Frontier molecular orbitals of *nido-OXD1* from IEFPCM-TD-B3LYP calculations (solvent: THF) at the lowest singlet excited state (S_1) optimized geometry (isovalue = 0.02).

Table S5. Molecular orbital energies (in eV) and contributions of moieties (in %) for *nido-OXD1* from IEFPCM-B3LYP calculations (solvent: THF) at the ground state (S_0) optimized geometry.

MO	Energy	OXD	Phenylene	<i>nido</i> -CB
LUMO+3	0.20	0.41	96.82	2.78
LUMO+2	0.19	0.11	97.21	2.68
LUMO+1	-0.44	32.10	61.47	6.43
LUMO	-1.15	39.46	55.34	5.20
HOMO	-5.03	6.06	15.91	78.02
HOMO-1	-5.12	0.50	4.60	94.91
HOMO-2	-5.55	20.73	40.46	38.81
HOMO-3	-6.11	3.58	43.81	52.61

Table S6. Molecular orbital energies (in eV) and contributions of moieties (in %) for *nido-OXD1* from IEFPCM-TD-B3LYP calculations (solvent: THF) at the lowest singlet excited state (S_1) optimized geometry.

MO	Energy	OXD	Phenylene	<i>nido</i> -CB
LUMO+3	0.20	0.15	96.62	3.23
LUMO+2	0.18	0.19	96.91	2.90
LUMO+1	-0.55	33.71	61.32	4.97
LUMO	-1.46	40.40	55.70	3.90
HOMO	-4.24	0.21	1.33	98.45
HOMO-1	-5.08	5.23	12.54	82.23
HOMO-2	-5.46	27.44	45.92	26.64
HOMO-3	-6.27	5.63	47.32	47.04

Table S7. Computed absorption and emission wavelengths ($\lambda_{\text{calc.}}$ in nm) and oscillator strengths ($f_{\text{calc.}}$) for *nido*-**OXD1** from IEFPCM-TD-B3LYP calculations at the ground (S_0) and lowest singlet excited state (S_1) optimized geometries.

Transition	$\lambda_{\text{calc.}}$ /nm	$f_{\text{calc.}}$	Major contribution
$S_0 \rightarrow S_1$	367.1	0.930	HOMO \rightarrow LUMO (95%)
$S_0 \rightarrow S_2$	351.2	0.028	HOMO-1 \rightarrow LUMO (97%)
$S_0 \rightarrow S_3$	319.6	0.728	HOMO-2 \rightarrow LUMO (96%)
$S_0 \rightarrow S_4$	295.9	0.029	HOMO \rightarrow LUMO+1 (93%)
$S_0 \rightarrow S_5$	290.2	0.094	HOMO-1 \rightarrow LUMO+1 (94%)
$S_1 \rightarrow S_0$	539.9 (423.1) ^a	0.044	HOMO \rightarrow LUMO (98%)

^a For the adiabatic transition corresponding to the 0–0 fluorescence.

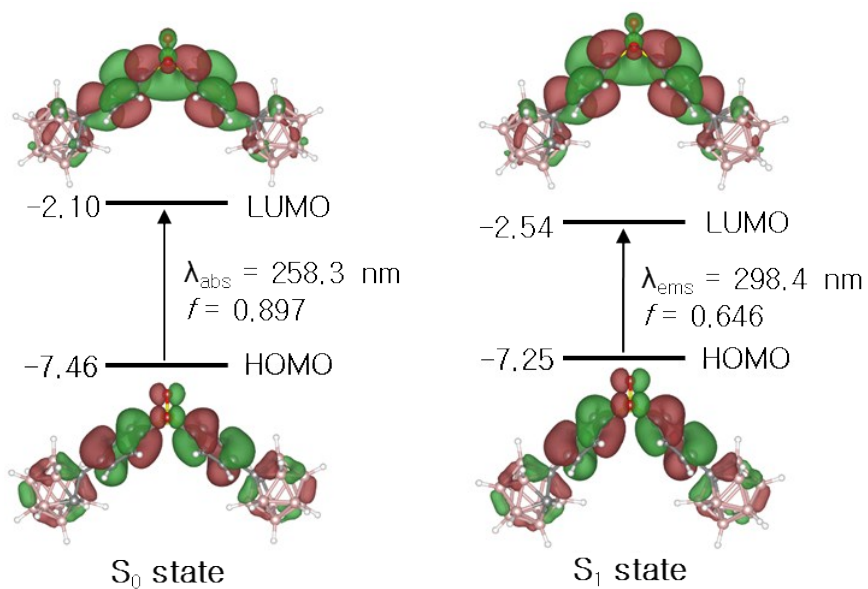


Fig. S19. Frontier molecular orbital diagrams and energies (eV) from DFT calculation (PCM in THF) of *closo-DPS1* (left) in the ground state (S_0) and (right) in the lowest singlet excited state (S_1) geometries. The transition energy (in nm) was calculated using the TD-B3LYP method.

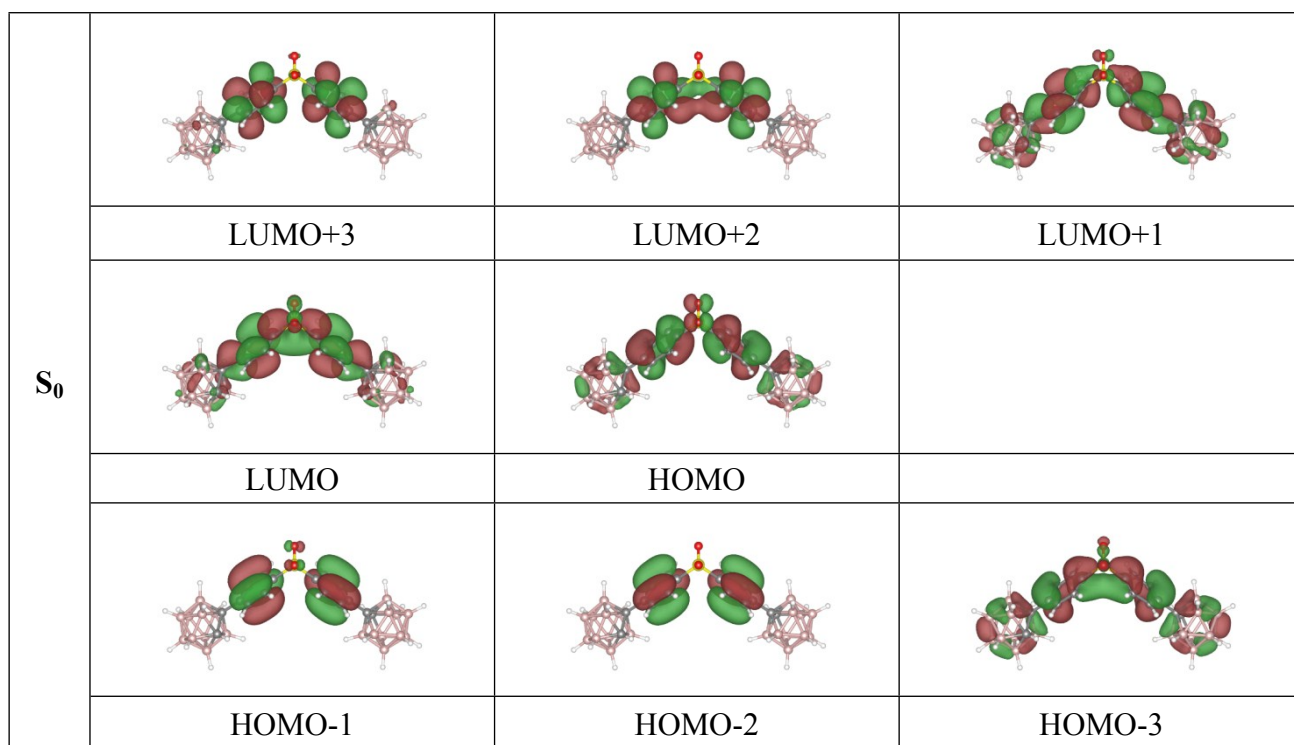


Fig. S20. Frontier molecular orbitals of *closo-DPS1* from IEFPCM-TD-B3LYP calculations (solvent: THF) at the ground state (S_0) optimized geometry (isovalue = 0.02).

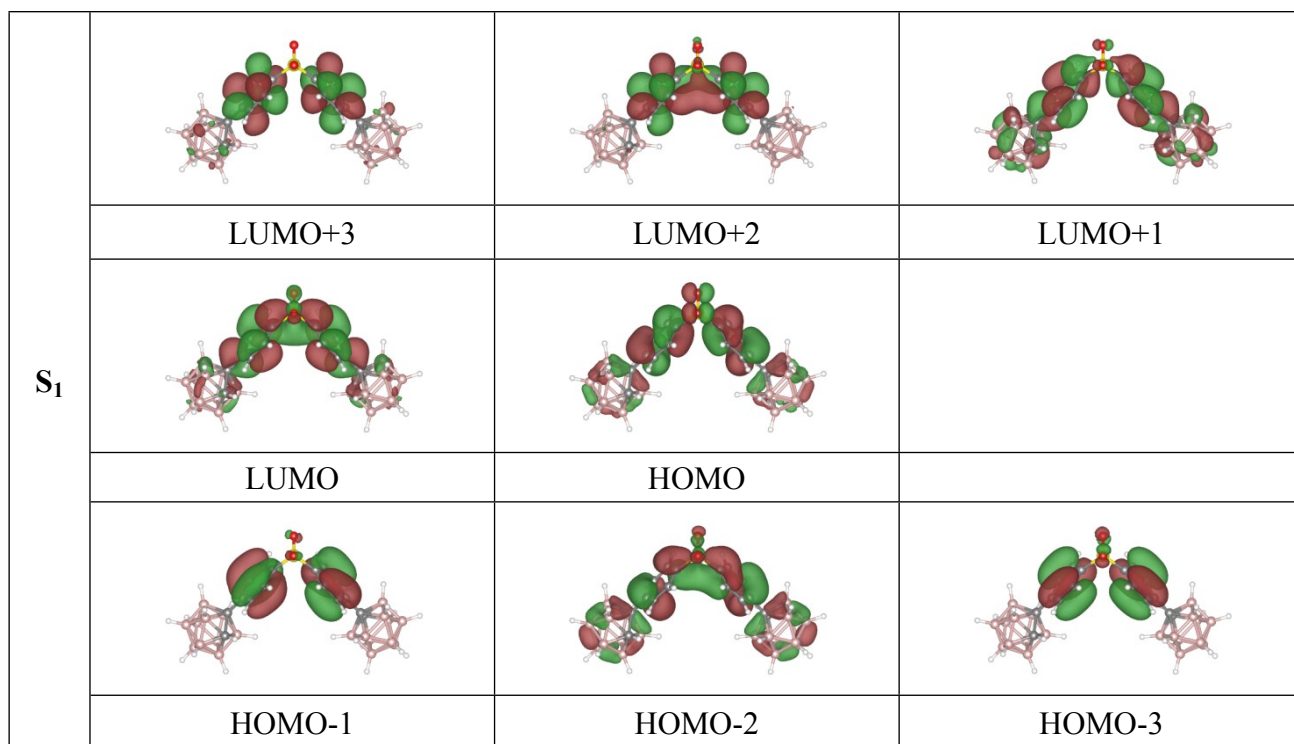


Fig. S21. Frontier molecular orbitals of *closo-DPS1* from IEFPCM-TD-B3LYP calculations (solvent: THF) at the lowest singlet excited state (S_1) optimized geometry (isovalue = 0.02).

Table S8. Molecular orbital energies (in eV) and contributions of moieties (in %) for *closo-DPS1* from IEFPCM-B3LYP calculations (solvent: THF) at the ground state (S_0) optimized geometry.

MO	Energy	Sulfonyl	Phenylene	<i>closo</i> -CB
LUMO+3	-0.95	0.22	91.12	8.66
LUMO+2	-1.19	0.57	93.24	6.20
LUMO+1	-1.41	2.68	70.01	27.32
LUMO	-2.10	8.82	77.50	13.68
HOMO	-7.46	5.41	81.39	13.20
HOMO-1	-7.72	1.20	97.56	1.25
HOMO-2	-7.81	0.06	98.65	1.29
HOMO-3	-7.99	3.35	73.78	22.87

Table S9. Molecular orbital energies (in eV) and contributions of moieties (in %) for *closo-DPS1* from IEFPCM-TD-B3LYP calculations (solvent: THF) at the lowest singlet excited state (S_1) optimized geometry.

MO	Energy	Sulfonyl	Phenylene	<i>closo</i> -CB
LUMO+3	-0.84	0.10	89.30	10.59
LUMO+2	-1.20	1.91	91.87	6.22
LUMO+1	-1.65	2.32	73.00	24.68
LUMO	-2.54	8.40	79.78	11.82
HOMO	-7.25	7.32	80.87	11.81
HOMO-1	-7.83	0.91	96.23	2.86
HOMO-2	-7.90	3.86	77.17	18.98
HOMO-3	-7.96	1.88	96.61	1.51

Table S10. Computed absorption and emission wavelengths ($\lambda_{\text{calc.}}$ in nm) and oscillator strengths ($f_{\text{calc.}}$) for *closo-DPS1* from IEFPCM-TD-B3LYP calculations at the ground (S_0) and lowest singlet excited state (S_1) optimized geometries.

Transition	$\lambda_{\text{calc.}}$ /nm	$f_{\text{calc.}}$	Major contribution
$S_0 \rightarrow S_1$	258.3	0.897	HOMO \rightarrow LUMO (98.5%)
$S_0 \rightarrow S_2$	252.9	0.001	HOMO-1 \rightarrow LUMO (77.3%) HOMO \rightarrow LUMO+2 (15.5%)
$S_0 \rightarrow S_3$	248.2	0.050	HOMO-2 \rightarrow LUMO (77.0%) HOMO \rightarrow LUMO+3 (12.2%)
$S_0 \rightarrow S_4$	232.7	0.097	HOMO-4 \rightarrow LUMO (97.4%)
$S_0 \rightarrow S_5$	230.1	0.097	HOMO-3 \rightarrow LUMO (87.6%)
$S_1 \rightarrow S_0$	298.4 (258.2) ^a	0.646	HOMO \rightarrow LUMO (98.9%)

^a For the adiabatic transition corresponding to the 0–0 fluorescence.

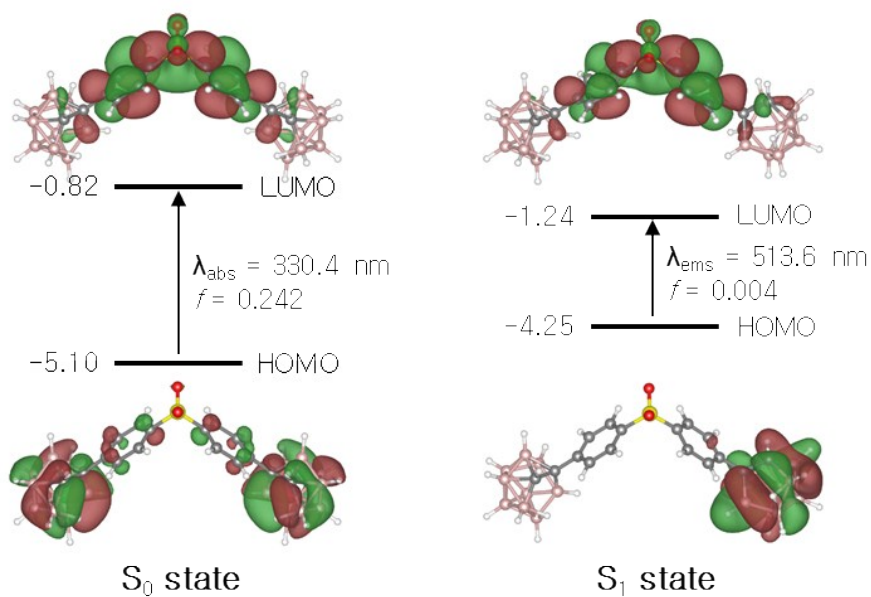


Fig. S22. Frontier molecular orbital diagrams and energies (eV) from DFT calculation (PCM in THF) of *nido-DPS1* (left) in the ground state (S_0) and (right) in the lowest singlet excited state (S_1) geometries. The transition energy (in nm) was calculated using the TD-B3LYP method.

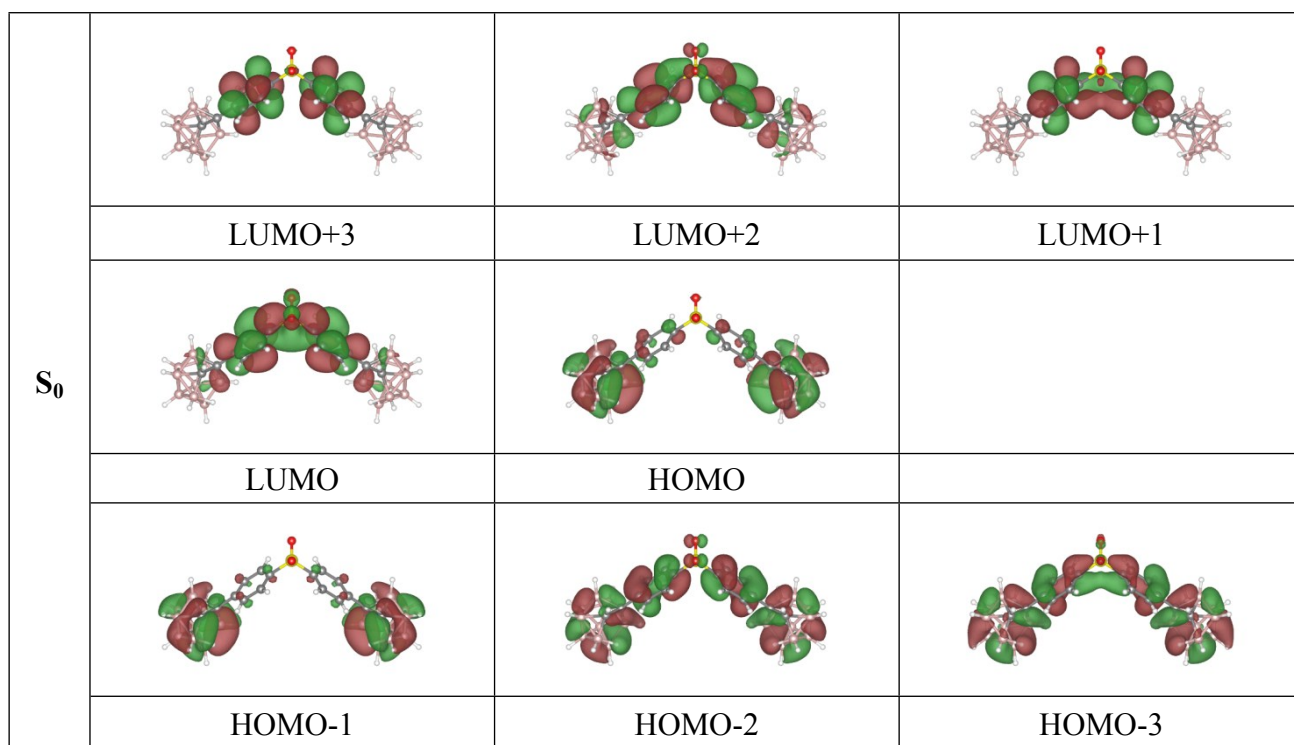


Fig. S23. Frontier molecular orbitals of *nido-DPS1* from IEFPCM-TD-B3LYP calculations (solvent: THF) at the ground state (S_0) optimized geometry (isovalue = 0.02).

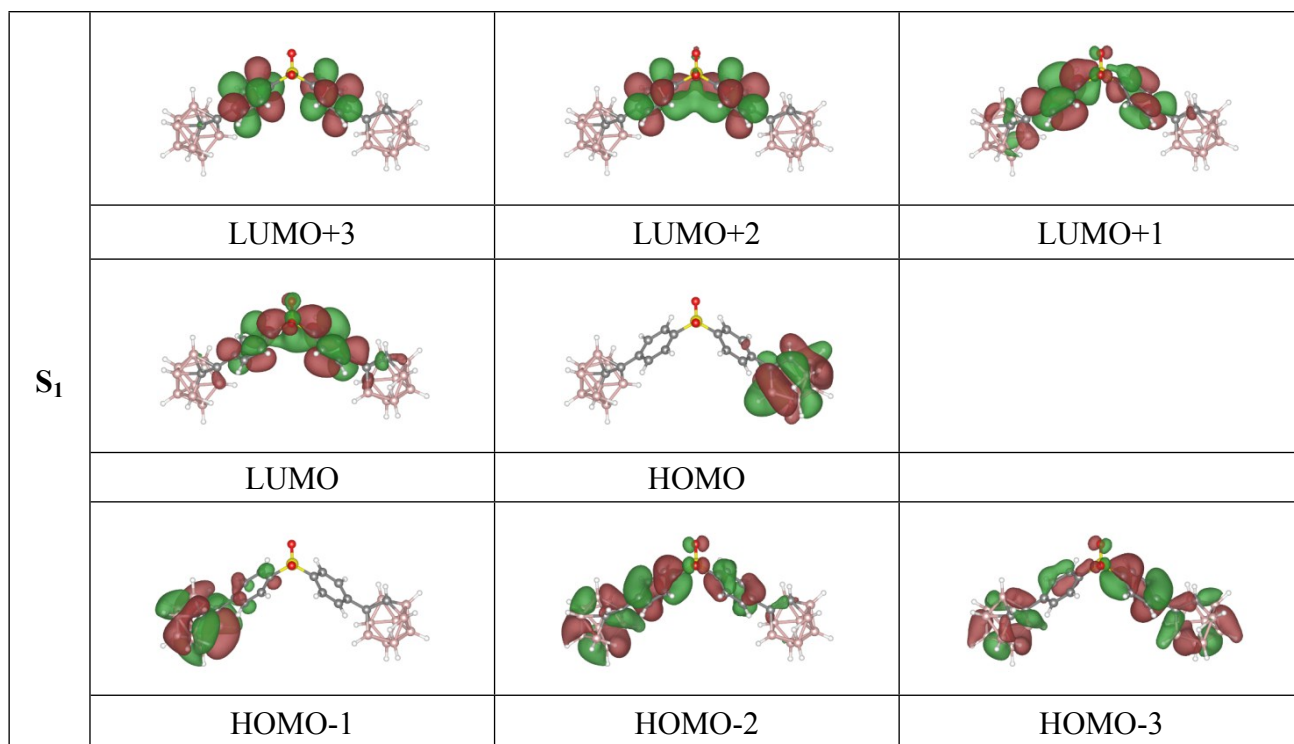


Fig. S24. Frontier molecular orbitals of *nido-DPS1* from IEFPCM-TD-B3LYP calculations (solvent: THF) at the lowest singlet excited state (S_1) optimized geometry (isovalue = 0.02).

Table S11. Molecular orbital energies (in eV) and contributions of moieties (in %) for *nido-DPS1* from IEFPCM-B3LYP calculations (solvent: THF) at the ground state (S_0) optimized geometry.

MO	Energy	Sulfonyl	Phenylene	<i>nido</i> -CB
LUMO+3	0.19	0.23	97.18	2.59
LUMO+2	0.01	4.43	84.32	11.25
LUMO+1	-0.06	0.73	97.01	2.27
LUMO	-0.82	11.40	80.88	7.72
HOMO	-5.10	0.24	6.97	92.78
HOMO-1	-5.13	0.21	3.72	96.06
HOMO-2	-5.96	1.86	51.45	46.69
HOMO-3	-6.24	1.65	35.08	63.27

Table S12. Molecular orbital energies (in eV) and contributions of moieties (in %) for *nido-DPS1* from IEFPCM-TD-B3LYP calculations (solvent: THF) at the lowest singlet excited state (S_1) optimized geometry.

MO	Energy	Sulfonyl	Phenylene	<i>nido</i> -CB
LUMO+3	0.18	0.18	97.20	2.62
LUMO+2	-0.07	1.39	96.36	2.24
LUMO+1	-0.17	4.34	86.93	8.73
LUMO	-1.24	11.86	82.80	5.33
HOMO	-4.25	0.01	0.78	99.21
HOMO-1	-5.12	0.22	4.64	95.14
HOMO-2	-6.07	3.36	55.06	41.58
HOMO-3	-6.54	3.01	49.59	47.40

Table S13. Computed absorption and emission wavelengths ($\lambda_{\text{calc.}}$ in nm) and oscillator strengths ($f_{\text{calc.}}$) for *nido-DPS1* from IEFPCM-TD-B3LYP calculations at the ground (S_0) and lowest singlet excited state (S_1) optimized geometries.

Transition	$\lambda_{\text{calc.}}/\text{nm}$	$f_{\text{calc.}}$	Major contribution
$S_0 \rightarrow S_1$	330.4	0.2416	HOMO \rightarrow LUMO (96.7%)
$S_0 \rightarrow S_2$	325.4	0.0783	HOMO-1 \rightarrow LUMO (96.9%)
$S_0 \rightarrow S_3$	278.8	0.0017	HOMO \rightarrow LUMO+1 (80.6%) HOMO-1 \rightarrow LUMO+3 (16.1%)
$S_0 \rightarrow S_4$	277.1	0.0063	HOMO-1 \rightarrow LUMO+1 (75.0%) HOMO \rightarrow LUMO+3 (22.9%)
$S_0 \rightarrow S_5$	270.5	0.6668	HOMO-2 \rightarrow LUMO (93.2%)
$S_1 \rightarrow S_0$	513.6 (374.2) ^a	0.0041	HOMO \rightarrow LUMO (98.1%)

^a For the adiabatic transition corresponding to the 0–0 fluorescence.